Arabian Journal of Chemistry (2020) 13, 8979–8994

King Saud University

Arabian Journal of Chemistry

www.ksu.edu.sa
www.sciencedirect.com

ORIGINAL ARTICLE

Selective CO_2 capture through microporous Tb $(BTC)(H_2O).(DMF)_{1.1}$ MOF as an additive in novel MMMs fabricated from Matrimid® 5218

Asma R. Tariq [a,b,*], Saadia R. Tariq [b], Misbah Sultan [a], Tariq Mahmud [a,*], Ghayoor A. Chotana [c]

[a] *Institute of Chemistry, University of the Punjab, P.O. Box 54590, Lahore, Pakistan*
[b] *Department of Chemistry, Lahore College for Women University, Lahore, Pakistan*
[c] *Department of Chemistry, Syed Babar Ali School of Science & Engineering (SBASSE), Lahore University of Management Sciences (LUMS), Sector U, DHA, Lahore Cantt 54792, Pakistan*

Received 28 August 2020; accepted 12 October 2020
Available online 24 October 2020

KEYWORDS

Metal organic frame works;
Matrimid®5218;
Mixed – matrix membranes;
Filler concentration;
Permeability;
CO_2/CH_4 selectivity

Abstract Mixed matrix membranes (MMMs) fabricated with porous metal organic frame works have enhanced the separation performance of polymer membranes. In this context microporous 3D Tb(BTC)(H_2O).$(DMF)_{1.1}$ MOF was incorporated into pristine Matrimid® with loadings of 10, 20 and 30 weight percentages. SEM micrographs indicated proper distribution of filler in the Matrimid and no interfacial voids were observed. Gas permeation studies evidenced the CO_2 permeability to be 13.2 (82.32%) and 18.34 (153.31%) and 25.86 Barrer for 10, 20 and 30 wt% MMMs respectively. The 257.18% increase in CO_2 permeability of 30 wt% MMM than methane was attributed to polar nature of CO_2, its smaller kinetic diameter, condensability, and larger solubility within the Matrimid matrix than non – polar and larger CH_4 molecules.

Addition of filler influenced the pure gas selectivity of all MMMs positively. So, 30 wt% MMM exhibited the highest 58.04% increase in selectivity that was attributed to the molecular sieving property of the filler and the size exclusion phenomena as followed by CH_4 and CO_2. The high values of mixed and pure gas selectivity were obtained upon increasing filler concentration. The commercial applicability of these MMMs was tested by checking their selectivity under increased feed concentrations of CO_2 and checking permeability and selectivities at high temperatures. The study depicted that, competitive sorption of gases, prevalence of size exclusion phenomena and polymer

* Corresponding authors.
E-mail addresses: asmartariq.9@gmail.com (A.R. Tariq), tariqm06@yahoo.co.uk (T. Mahmud).
Peer review under responsibility of King Saud University.

Production and hosting by Elsevier

https://doi.org/10.1016/j.arabjc.2020.10.021

chains relaxation at higher temperature were responsible for low gas selectivity. MMM with 30 wt% of MOF lied close to Robson's Upper bound 2008 that indicated its good separation potential.

1. Introduction

The worldwide annual emission of CO_2 and methane gas is increasing enormously due to burgeoning population, unplanned industrialization and combustion of fossil (Pall et al., 2011). CO_2 causes ocean acidification and is responsible for climate change as well (Moghadam et al., 2017; He et al., 2014). The use of renewable energy sources including hydrogen as a substitute for the fossil fuels may help in controlling the exceedingly increasing CO_2 emissions (Rehman et al., 2019). The conventional techniques used for the removal of these gases such as cryogenic distillation (Wang et al., 2017), amine based wet scrubbing, use of activated carbon or carbon molecular sieves (Shafeeyan et al., 2015) etc. have been found to be associated with large energy deficit. This motivated the researchers to focus their attention on membrane technology, that is not only energy efficient but also environment friendly and cost effective one (Marti et al., 2018; Rezakazemi et al., 2018).

The material used for the fabrication of the membrane governs its performance (Vinoba et al., 2017). Polymer based membranes exhibit the characteristics of ease of preparation and process ability so they find broad range of applications in efficient gas separations. So, PBI, Polysulfone, cellulose acetate, polyimide and polyethersulfone have been widely explored in this field due to their high mechanical strength and ability to form defect – free thin layers with cross – linking ability (Abdulhameed et al., 2017; Hu et al., 2016a). These glassy polymers also exhibit intrinsic microporosity and high free volume. However, their adherence to the surface of filler particles is not remarkable (Anjum et al., 2015). Thus polymer based membranes offer limited selectivity and reduced permeability due to plasticization effect under harsh conditions of increased feed pressure and CO_2 concentration. Moreover, they are associated with fouling and structure instability at elevated temperatures. All these factors have limited the commercialized use of these membranes for CO_2 separation (Basu et al., 2010a, 2010b, Mubashir et al., 2017). In order to realize the commercial use of polymer based membranes for separation and/or storage of CO_2 and CH_4, they must exhibit a minimal environmental foot – prints with adjunct cost efficacy and should be efficient enough to surpass the quantified selectivity – permeability trade – off (Robeson, 1991, 2008).

Membranes based on inorganic materials such as silica (Kim et al., 2001), zeolite (Venna and Carreon, 2011) and carbon molecular sieves (Yamamoto et al., 1997) have been extensively explored for their potential for CO_2 separation from natural gas and N_2 due to their high thermal stability (Mubashir et al., 2015). However, their drawbacks such as difficult fabrication process, high cost and brittleness have limited their use (Ismail et al., 2011).

In order to exploit the polymer materials for efficient separation performance, the introduction of MMMs offers a promising substitute for extensive use of facilitated transport membranes, thermally re – arranged polymers (Wolińska-Grabczyk et al., 2017) chemical modification (Tin et al., 2003), blending (Mannan et al., 2013) and cross – linking (Kertik et al., 2017). However, fabricating a defects free MMMs still remains a challenge. A proper selection of filler – polymer pair may overcome this problem and thus efficiency of MMMs may be improved (Chung et al., 2007) That is why, researchers usually use varying particle size and shape (Anjum et al., 2015) percent loadings, surface modification of fillers (Venna et al., 2015) and an immense variety of organic (Goh et al., 2011) as well as inorganic porous materials for fabrication of MMMs so that efficient gas separation module could be designed (Song et al., 2012; Li et al., 2013).

The materials that have been explored for the fabrication of MMMs include: activated carbons (He et al., 2018, Khan et al., 2012a), carbon molecular sieves (CMSs) (Ward and Koros, 2011), carbon nano tubes (CNTs) (He et al., 2018), silica (Ariazadeh et al., 2020), Zeolites (Castruita – de León et al., 2020), TiO_2 nanoparticles and MOFs (Li et al., 2017).

MOFs are built by an appropriate combination of metal ions with polyfunctional organic connectors. Their tunable porous structure and high flexibility render them highly suitable for separation applications (Li et al., 2011; McGuire and Forgan, 2015). Their high thermal stabilities, high surface areas (up to 7000 m^2/g), structural diversity and strong adsorption affinities, are the additional characteristics to this effect (Cota and Martinez 2017). Recently, the doping of metal organic frameworks with ionic liquids have explored their wide applications in catalysis (Cota and Martinez, 2017; Hu et al., 2020). They have also been used in separations (Shan et al., 2018), in luminescence (Lian et al., 2020), drug delivery (Johannas et al., 2020), and as sensors (Yang et al., 2020).

The metal – organic frame works offer superior affinity with the polymer matrix. Thus a good compatibility between the filler and the polymer phase produces better inorganic – organic phase adhesion. Resultantly, the membranes free from interfacial voids are formed which not only have improved performance but they may also surpass the Robeson's upper bound (Robeson, 2008; Venna and Carreon, 2015).

The first report on MMMs dates back to 1970′s when a rubbery polymer PDMS was fabricated by using zeolite 5A (Liu et al., 2018). Good compatibility between filler and the polymer was evidenced in PBI based MMMs fabricated with nanoparticle size UiO-66(Hf) - $(OH)_2$ MOFs (Hu et al., 2016a). The pore sizes and BET surface (922 $m^2\ g^{-1}$) area of UiO − 66(Hf) - $(OH)_2$ were reduced (~4 Å) as compared to their UiO-66(Zr), analogues due to heavier Hf cations and somewhat bulkier linkers. The fabrication of PBI matrix with 10 wt% loading of this MOF yielded excellent gas separation performance (Hu et al., 2016a).

Similarly, a number of MOF – polymer pairs have been explored for the selective separation of CO_2 from mixtures of other gases. The PSf based MMMs fabricated with micro – mesoporous silica (MSS)/ZIF – 8 composite were also are reported for their improved gas permeability. However, no sig-

nificant change in selectivity was observed even at 32 wt% loading of the filler (Sorribas et al., 2014). The increased free volume of ZIF – 8/PSf MMM was shown to be responsible for excellent H_2/CH_4 and O_2/N_2 separations (118 and 8.3 respectively) (Ordoñez et al., 2010).

Similarly, the PSf based MMMs fabricated with HKUST-1, ZIF-8, and Silicate-1, were tested for CO_2/CH_4 separations, in these cases increased gas permeability was observed at the cost of decreased CO_2/CH_4 selectivity (Zornoza et al., 2011).

Matrimid ® is a high performance glassy polymer that possesses better mechanical properties, good processability, high chemical and mechanical resistance, high free volume and better CO_2 - philic sites. That is why it is favored for gas separation studies (Venna et al., 2015). Many researchers have been involved in fabricating the Matrimid based MMMs while incorporating different fillers to study the increase in separation factor for H_2, CO_2 and CH_4. For example, polyimides (PI) added with 15 wt%. loading of MIL – 53 exhibited an 84% increase in ideal selectivity of CO_2/CH_4 (Dorosti et al., 2014). Similarly, Matrimid® fabricated with 30 wt% loading of $Cu_3(BTC)_2$ yielded a 121% increasd permeability of CO_2 (Liu et al., 2009) as compared with pristine Matrimid® membrane with no change in selectivity. Song et al. (2012) reported that a 30 wt% loading of ZIF – 8 into the Matrimid® resulted in a drastic increase in CO_2 permeability without any loss of selectivity. The extra free volume in the ZIF – 8/Matrimid® MMMs was responsible for improved permeability of MMMs (Ordoñez et al., 2010).

In case of ZIF – 12/ Matrimid MMMs, the increased MOF loading was observed to cause polymer rigidification around the particles and thus selectivity was increased with loss of permeability for CO_2/CH_4 mixture (Boroglu et al., 2017). Similarly, NH2-MIL-53(Al)/6FDA-DAM MMM exhibited a 76.9% increased selectivity for CO2/CH4 (Tien-Binh et al., 2015).

Lanthanide based MOFs have the advantages of flexible coordination geometry with porous frame works over the transition metals (Silva et al., 2010; Feng et al., 2010) but have the disadvantage of a less control over their final topology. The examples of these microporous structures include 3D coordination polymers (CPs) of Erbium(III) ion that was prepared by using 1, 3, 5 – benzenetricarboxylic acid (BTC) linker. The MOF exhibited a BET surface area of 259 m^2/g (Łyszczek et al., 2017). Similarly, Ln(BTC)(H_2O) $(DMF)_{1.1}$ MOFs where Ln = Er, Y, Yb and Tb (III) ions have also been reported (Jiang et al., 2010). The high surface area of all these MOFs (in the range of 676–1080 m^2/g) suggests their potential application in H_2 storage.

LaBTB/6FDA–DAM polyimide MMMs were shown to cross the 2008 Robeson upper-bound and exhibited reduced plasticization effects. It also exhibited a stable CO_2 permeability of 700 barrer and CO_2/CH_4 selectivity of 30 within 120 h (Hua et al., 2018).

Benzene – 1, 3, 5 – BTC have been immensely explored as a linker for the design of porous MOFs (Łyszczek et al., 2017). MOF – 76 (Tb) possesses the properties of a molecular sieve as evidenced from its sorption isotherms for different gases like N_2, CH_2Cl_2, Ar, C_6H_6 and C_6H_{12} (Rosi et al., 2005). Similarly, Y – BTC has been reported to be highly selective for sorption of H_2 against N_2 due to the presence of tetragonal pores of approximately 6 Å in its framework (Luo et al., 2008).

Porosity, chirality and stability are the important factors that decide the role of a compound in chemistry, catalysis and biology, but, it is quite difficult to fabricate a material that exhibits all these characteristics (Davis, 2002). Tb(BTC)(H_2O).$(DMF)_{1.1}$ is a enantiomerically pure, highly thermostable, 3D chiral, MOF with high surface area of 786 m^2/g, and a permanent porosity. It also possesses free windows of 6–7 Å where metal sites are quite accessible. Tb (IIII) ion itself is luminescent (van Krevel et al., 2002). This MOF may render excellent potential for H_2 storage (Jiang et al., 2010) as well as in the field of catalysis and gas storage (Jiang et al., 2010).

The proper selection of a porous lanthanide based MOF as a filler in the polyimide matrix for fabrication of MMMs may improve the selectivity and permeability of the MMMs. Considering these facts, the present work was designed that is based on the synthesis of a enantiomerically pure, 3D chiral, and microporous MOF exhibiting high surface area for fabrication of 10, 20 and 30 wt% Tb(BTC)(H_2O).$(DMF)_{1.1}$/Matrimid5218® MMMs. The obtained MMMs were tested for CO_2 permeability and selective separation of CO_2 from CO_2/CH_4 gas pair. To the best of our knowledge, this is the first investigation on use of microporous Tb(BTC)(H_2O).$(DMF)_{1.1}$ MOF as filler in Matrimid® based MMMs for selective separation of CO_2.

2. Materials and methods

2.1. Chemicals

The analytical grade solvents and reagents obtained from commercial suppliers were used for present study without any further purification. Matrimid 5218® was provided by Marjan Polymer Industries Pakistan after import from Ciba Specialty Chemicals North America. Prior to casting the membranes, The Matrimid® 5218 was pre – dried in a vacuum oven set at 120 °C. Acetone and chloroform procured from BDH (England). Analytical grade Methanol and dichloromethane were imported from E Merck (Germany). Benzene – 1, 3, 5 – tricarboxylic acid (95% pure), $Tb(NO_3)_3{\cdot}5H_2O$ (99.9%, trace metal basis), were obtained from Sigma Aldrich.

2.2. Preparation of MOF

The highly thermostable 3D microporous [Tb(BTC)(H_2O).$(DMF)_{1.1}$] MOF with high surface area was prepared by following the procedure published elsewhere (Jiang et al., 2010). For this purpose, a mixture of BTC (0.25 mmol) and Tb$(NO_3)_3{\cdot}6H_2O$ (0.5 mmol) was sealed in a Teflon – lined reactor of 24 mL capacity along with DMF (4 mL), and H_2O (4 mL) as solvents. Pure colorless needle like crystals were obtained after heating at 105 °C for 24 h. The solvent was removed from the prepared MOF by using a sterile and dried syringe. Subsequently, the unreacted impurities were removed from this MOF by using solvent exchange technique by employing a mixture of 1:1 DMF and water. The obtained material was first air dried and then dried under vacuum at 180 °C for 36 h to make it completely free from solvent and to activate it, so that it may be used for preparing MMM (Jiang et al., 2010).

2.3. Fabrication of membranes

The chemical structure of Matrimid®5218 is shown in Fig. 2.

The pure Matrimid®5218 membrane was fabricated by adopting solution casting technique. Prior to use, Matrimid®5218 was dried for 24 h at 110 °C in a vacuum oven. A viscous 3.5% solution of Matrimid prepared in chloroform was poured into a flat surface glass Petri plate for controlled evaporation. The MMMs with different filler loadings were then prepared and compared with pure Matrimid®. The MOFs were crushed finally in a pestle and mortor before fabrication of the MMM so that their nice distribution within the polymer matrix may be ensured and agglomeration is avoided. The Matrimid was stirred for 24 hrs in chloroform at room temperature.

In order to improve the compatibility at the filler/polymer interface. A precise "priming protocol" was adopted. The MOF suspensions of 10%, 20% and 30% by weight loadings were prepared in accordance with the following equation:

$$Filler\ \ loading\ \ (weight\%) = \left[\frac{wt.of\ \ filler}{wt.of\ \ polymer + wt.of\ \ filler}\right] \times 100 \tag{1}$$

The MOF solution was introduced with 20% of whole Matrimid solution and then stirred and sonicated for 5–10 min. A batch wise (20 wt%) addition of the residual polymer solution was carried out to the MOF solution. After the addition of every batch of residual polymer solution to MOF suspension, continuous shaking for 2 h and sonication (10–15 min) is carried out. This procedure was continued until all the polymer solution was added to MOF suspension. The obtained viscous polymer/MOF solution was cast on flat surface glass Petri plate placed on a balanced, flat surface at room temperature. A general representation of the resultant MMMs can be seen in Fig. 1 where by the transport of gases (CO_2 and CH_4) in their mixture is explained. The membranes were finally cured at 140 °C and then stored in vacuum dessicator before further characterization and studies.

2.4. Characterization of filler and MMMs

The specific functional groups of the MMMs was identified by the Agilent Cary 630 ATR – FTIR spectrophotometer that was equipped with diamond crystal. The spectra were recorded in scanning range of 4000–400 cm^3 at 64 scans per seconds. No specific sample preparation was required for the MMMs. A small piece of MMMs was nicely cut with Teflon lined pair of scissors and carefully placed on ATR – FTIR for recording the spectrum.

The Bruker D2 Phaser, desktop diffractometer was used to record the diffractograms of the synthesized MOF and MMMs samples with Cu Kα radiations (λ = 1.542 Å). The 2θ range of 3 to 60° was used for the PXRD measurements of finally crushed MOF powder.

Thermal Analyzer, SDT Q600 was used to record the measurements of weight changes (TGA) as a function of temperature (room temperature to 1000 °C) in pre – dried and annealed filler and MMMs in N_2 atmosphere purged at flow rate of 20 mL/min with a ramp of 10 °C/min.

SEM images of the MOF particles and the MMMs were obtained from a FEI Nova 450 Nano SEM to know about the surface morphology of the samples at variable pressure. In order to obtain a more conductive and additionally receptive surface of the samples, non crushed MOF crystals [Tb(BTC)(H_2O).$(DMF)_{1.1}$] and 10 wt% MMM were sputtered coated with gold particles. It would also entail a high surface sensitivity at varying magnifications in order to obtain ultra-high resolution at high – and low – voltage under ideal operating conditions.

2.5. Activation of MOF

The MOF was subjected to solvent exchange first by soaking it in methanol for more than 24 h and then transferring it to dichloromethane for 24 h. It was followed by evacuation and simultaneous heating at 180–350 °C for 36 h. The sample was stored under argon (Ar) environment to avoid contact of moisture and dust (Jiang et al., 2010).

2.6. Gas permeation studies

The gas separation performance of membranes was tested under isochoric conditions for CH_4 and CO_2 as single components and binary mixtures by using a specified gas separation unit as shown in Fig. 3.

The working of the gas separation set – up has been reported earlier (Khan et al., 2010). The GC coupled with a TCD (thermal conductivity detector) was used to determine the composition of feed and permeate gases. Inside the GC, Ar was used as the carrier gas for the sample. A pressure transducer of 10 Bar was attached to a constant volume auxiliary cylinder.

In order to measure the pure gas components, the individual gases (CO_2 and CH_4) were allowed to passed through the membrane's module and the gas permeability calculations were performed by allowing the gas to expand in an auxiliary cylinder. The following equation was used to determine the rate of pressure increase with time:

$$P_i = \frac{273 \times 106}{760} \frac{V}{AT(76/14.7)P_2}\left(\frac{dP}{dt}\right) \tag{2}$$

where V represented the cylinder volume (cm^3), A is the membranes surface area (cm^2), T shows the feed temperature on Kelvin scale, (dP/dt) denotes the rate of pressure change (mmHg/s) and po shows the upstream feed pressure in mmHg.

The coefficient of permeability (in practical unit of Barrer) is measured by the equation given below

$$1Barrer = 10^{-10}\frac{cm^3STP.cm}{cm^2.s.cmHg} = 3.35 \times 10^{-16}\frac{mol.m}{m^2.s.Pa} \tag{3}$$

The ideal selectivity of pure gas was determined in terms of the ratio of the gas permeabilities as given by the Eq. (4).

$$Selectivity = Pi/Pj \tag{4}$$

The feed gas mixtures were prepared by using the mass flow controllers (Sierra Instruments, USA). The feed mixture was injected into the membrane module at 1 L/min and the permeate was collected. An online gas chromatograph was used to analyze the composition. The gas was allowed to expand inside

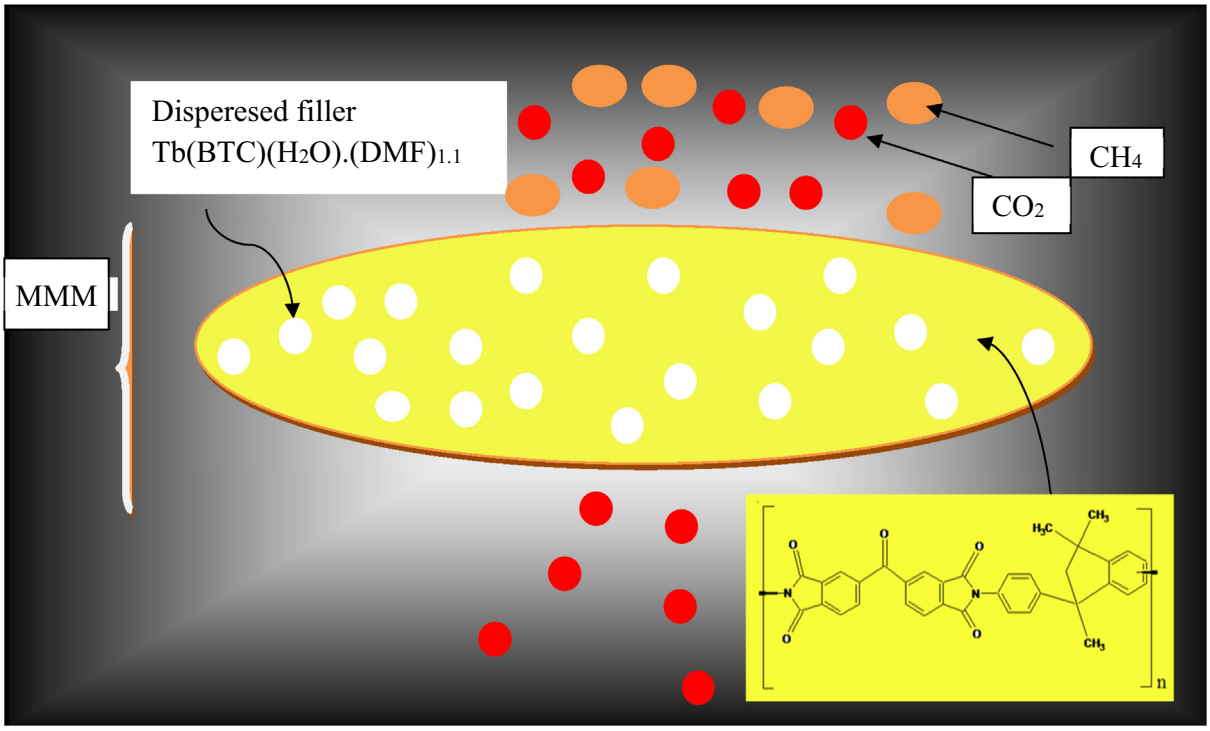

Fig. 1 Graphical Abstract representing selective transport of CO_2 through the MMM.

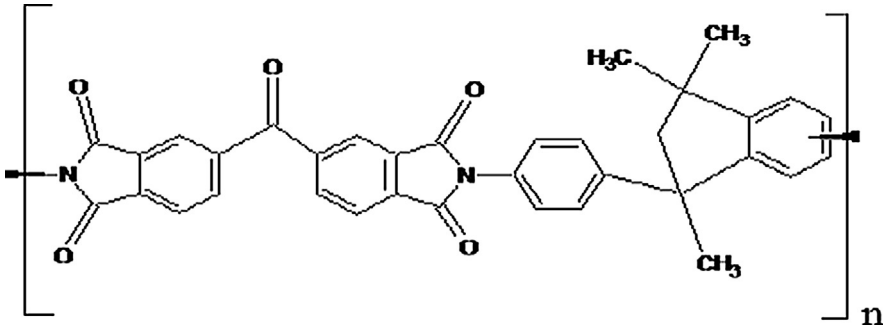

Fig. 2 Chemical Structure of Matrimid (a polymer of 3, 3′, 4, 4′ – benzophenone tetracarboxylicdianhydride and diaminophenylindane units).

an auxillry cylinder to inspect the gas permeability and the rate of pressure increase was measured with time. The permeability of the mixed gases was calculated by using the Eq. (5).

$$P_i = \frac{273 \times 106}{760} \frac{y_i V}{AT(76/14.7)x_i P_2}\left(\frac{dP}{dt}\right) \quad (5)$$

where *xi* and *yi* are the mole fractions of upstream and downstream components i respectively, *V* in units of cm^3 shows the constant volume of container, A is the surface area of membranes in units of cm^2, T represents the temperature in Kelvin scale (K), the rate of change of pressure is depicted by (dP/dt) in terms of mmHg/s, the upstream pressure alternatively called feed pressure in mmHg is represented by p_o.

The mole fractions of feed mixture and permeation compositions were used to measure the mixed gas selectivity, as provided in the Eq. (6).

$$a_{ij} = \frac{y_i/y_j}{X_i/xX_j} \quad (6)$$

The solution – diffusion mechanism governs the transport through the polymeric membranes, as explained by the following equation

$$P = DS \quad (7)$$

where D and S represent the diffusion and solubility coefficients respectively, while, P is the gas permeability. The time – lag method was used to determine the diffusion coefficient (d) where the expansion of permeate gas was allowed through an auxiliary constant volume cylinder that was attached with a pressure transducer. One side of the auxiliary cylinder directs the test gas whereas the other side creates the vacuum. The expansion of the gas was then allowed inside the auxiliary cylinder in the absence of vacuum and a pressure transducer was used to note the rate of pressure increase with time. A steady state of permeate from the membranes was established, and subsequently, the rate of increase in gas pressure was plot-

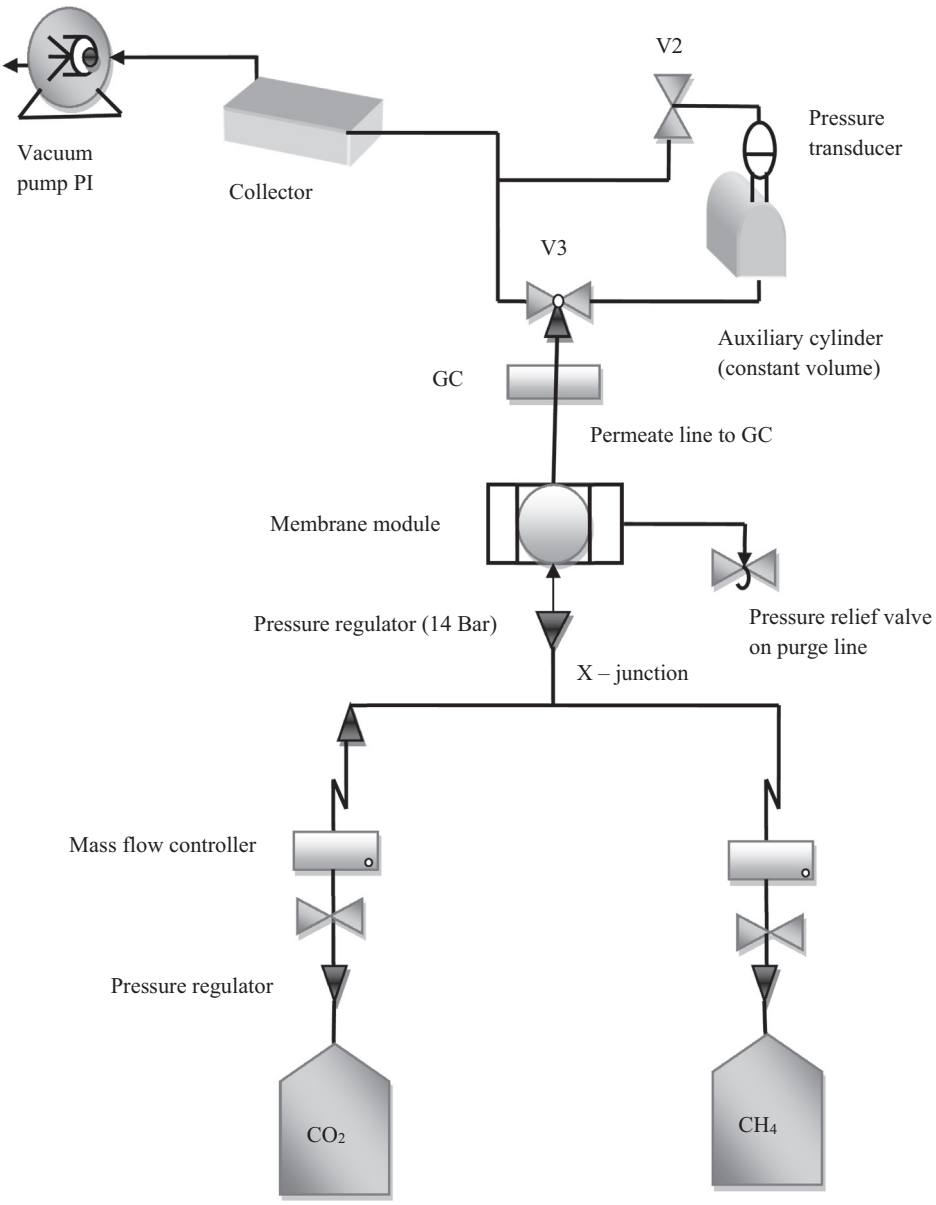

Fig. 3 Illustration of a gas separation unit.

ted to calculate the time – lag intercept θ. The time lag method was also used to measure the diffusivity through the equation

$$D = l^2/6\theta \quad (8)$$

where l shows the thickness of membrane and θ is the time – lag (Galiatsatou et al., 2006). In order to measure the apparent solubility of gases in the membrane, Eq. (9) was used:

$$S = P/D \quad (9)$$

3. Results and discussion

3.1. Characterization of $Tb(BTC)(H_2O).(DMF)_{1.1}$ MOF

Terbium belongs to member of heavy lanthanide group with high coordination number. In this MOF, terbium- (III) ion is coordinated with six oxygen atoms from six carboxylate groups of six BTC ligands and one oxygen atom from the terminal water molecule forming a distorted pentagonal-bipyramidal structure. This (6, 6) coordination produces 3D chain, helical framework with 6 – 6 $Å^2$ and 7 – 7 $Å^2$ along c axis. This MOF crystallizes in tetragonal crystal system and in $P4_322$ space group (Jiang et al., 2010].

Fig. 4a depicts the FTIR spectrum of the MOF. The FTIR spectrum of this MOF clearly shows that the free acid form of H_3BTC ligand was not present in the MOF powder complex rather its deprotonated form existed, as no vibrations were observed at, 1676 cm^{-1} (OCOOH), 1720 cm^{-1} and 2658. The association of lanthanide ion with the carboxylate group was evidenced by the appearance of a weak vibrational frequency at 1615 cm^{-1} and a sharp, high energy asymmetric (ν_{as}(C—O)) stretching frequency at 1543 cm^{-1}. Further, strong and sharp peak at 1379 cm^{-1} was assigned to the symmetric (ν_{as}(C—O)) stretch of carboxyl groups. The presence of these two sets of

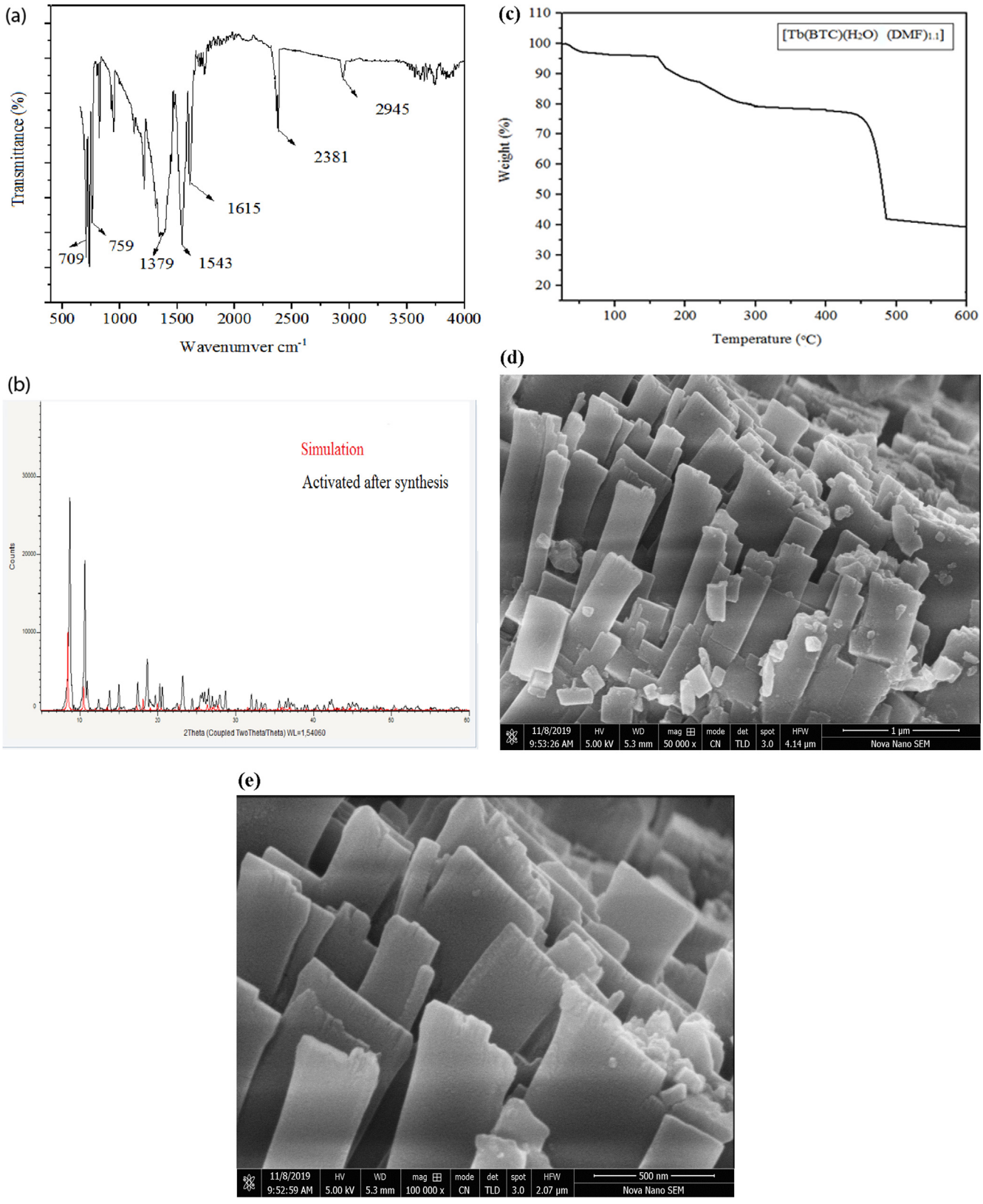

Fig. 4 Characteristic FTIR peaks (a) PXRD pattern (b) TGA of as prepared $Tb(BTC)(H_2O)$ $.(DMF)_{1.1}$ (c) SEM micrograph showing rod shaped morphology (d and e).

stretching frequencies confirms the presence of the dicarboxylate ion in the sample. The aromatic benzene ring stretch appeared at 2945 $cm^{-1,}$ while the out of phase skeletal bending vibration of the benzene ring appeared at 759 cm^{-1} and 709 cm^{-1} (Guo et al., 2006; Łyszczek, 2007; Łyszczek et al., 2011). The absence of broad band at 3400 cm^{-1} in the FTIR

spectra of MOF evidenced the absence of any coordinated or hydrogen bonded water molecule in the MOF system. It was due to the fact that the sample was activated by employing both the thermal and solvent treatments. Further, the absence of vibrations at 1711 cm^{-1} characteristic of DMF showed that DMF was not a part of the system (Jiang et al., 2010)

The simulations of the X-ray diffractograms with the originally produced [Tb(BTC)(H_2O).$(DMF)_{1.1}$] MOF's was performed and depicted the in 4(b). The Fig. 4(b) showed that the XRD pattern of the original and the as synthesized but activated [Tb(BTC)(H_2O).$(DMF)_{1.1}$] MOF were well simulated (Jiang et al., 2010). The 2θ value of 8.8° and 10.9° for the MOF were assigned to the maximum intensity peaks. Diffractograms at 2θ position 12.5° and 18.5° were also present.

The obtained PXRD patterns indicated the formation of MOF in pure phase while its crystalline nature was indicated by the narrow and sharp peaks (Jiang et al., 2010).

All the XRD patterns observed were quite similar to the known bulk phase of [Tb(BTC)(H_2O).$(DMF)_{1.1}$] (Jiang et al., 2010) evidencing the two to be isostructural. The bulk phase crystallinity was observed even after activation, but with a small shift in diffraction patterns toward the right due to the smaller radius of Tb^{3+} ion that further indicated a certain degree of framework flexibility and shrinkage.

Thermogram (TGA) of the activated MOF sample recorded in temperature range of 25 °C to 1000 °C is provided in Fig. 4c. The thermogram indicated a very high thermal stability of the Tb MOF. At a temperature of about 315–345 °C, the MOF released its terminal water and free DMF molecules thereby producing guest – free Ln(BTC) frameworks. After that, a long plateau appeared up to 450 °C and then degradation of the MOF framework took place (Jiang et al., 2010).

The cross sectional SEM micrographs of the as synthesized, needle like activated [Tb(BTC)(H_2O).$(DMF)_{1.1}$] MOF crystals are shown in Fig. 4(d and e) at different magnifications. The figure depicted the formation of needle like crystals of the MOF with different sizes (Jiang et al., 2010). These needles were then further stacked together. It is noteworthy that the MOF sample used for inclusion in mixed matrix membrane were finely ground prior to use, so there was no need to measure the sizes of the synthesized crystals in the framework. However, SEM micrographs were recorded without grinding the MOF crystals as mentioned before.

3.2. Characterization of MMMs

The ATR-FTIR spectra of pure Martimid and MMMs with different Wt % loadings are presented in Fig. 5. The spectrum for pure Matrimid®5218 membrane showed characteristic symmetric stretch for C = O group of polyimide at1777 cm^{-1} while it was at 1780 cm^{-1} for the MMMs. Their corresponding asymmetric stretch were observed at 1713 and 1717 cm^{-1}. The C—N stretch of imide group of Matrimid®5218 was obtained as sharp absorption band in the region 1354–1362 cm^{-1}(Anjum et al., 2015). The stretching frequencies of aromatic double bond were observed at 1506–1514 cm^{-1} (with slight shift towards higher wave number) and 1611–1612 cm^{-1} (with slight shift towards lower wave number) in the MMMs. The imidic group of pristine Matrimid® 5218 observed at 1671–1675 cm^{-1} was shifted towards lower wave number range in MMMs.

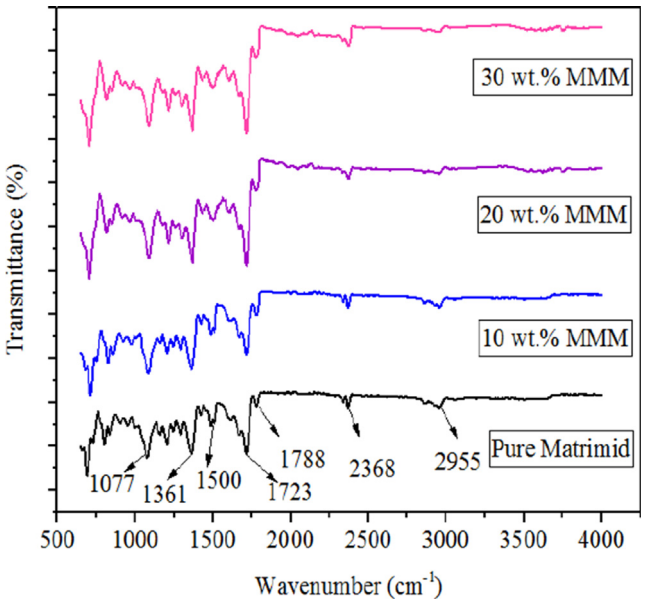

Fig. 5 FTIR spectra of pure Matrimid membrane and MMM with 10 wt% loading of filler [TbBTC(H_2O).$(DMF)_{1.1}$] MMM with 20 and 30 wt% loading of the filler.

The Fig. 6 (a) and 6 (b) depicts the PXRD patterns of the pristine Matrimid membrane and MMMs with different weight % loadings respectively. The high intensity 2θ peak observed at 16° in pure Matrimid was weakened in the MMMs due to the disruption of primary structure of Matrimid (Ahmad et al., 2013). The incorporation of different amounts of fillers in MMMs led to the different intensities of diffractograms. While, the crystallinity of the filler was not affected on incorporation into the Matrimid matrix.

The thermograms for the MMMs are given in Fig. 7. It was noted that all of the MMM followed the same trend of weight loss on thermogram. The slowest weight loss was exhibited by 20 wt% MMM while all of the membranes were found to be stable at up to 500 °C with a major weight loss observed at 500–650 °C.

The MMM with 10 wt% MOF loading was used to investigate the morphology of the membrane.

The Fig. 8(a) clearly exhibited a needle like morphology of the MOF as was note in the SEM micrographs of MOF that was found in agreement with the previously reported crystal structure and PXRD patterns (Jiang et al., 2010). The Fig. 8 (a) also depicted a homogeneous distribution of [Tb(BTC)(H_2O).$(DMF)_{1.1}$] MOF in the Matrimid®5218 matrix while the two phases remained distinct. No agglomeration of MOF was observed and the polymer – MOF interface exhibited no prominent non selective voids. The membranes were flexible enough to offer easy handling. The SEM micrographs revealed the presence of sufficient filler – polymer interactions at their interface resulting in specific control over the outer surface of MOF that were attributed to the hybrid nature of the MOF. The Fig. 8(b) depicts the surface image of the same MMM indicating the needle like MOF crystals are covered nicely within the Matrimid matrix.

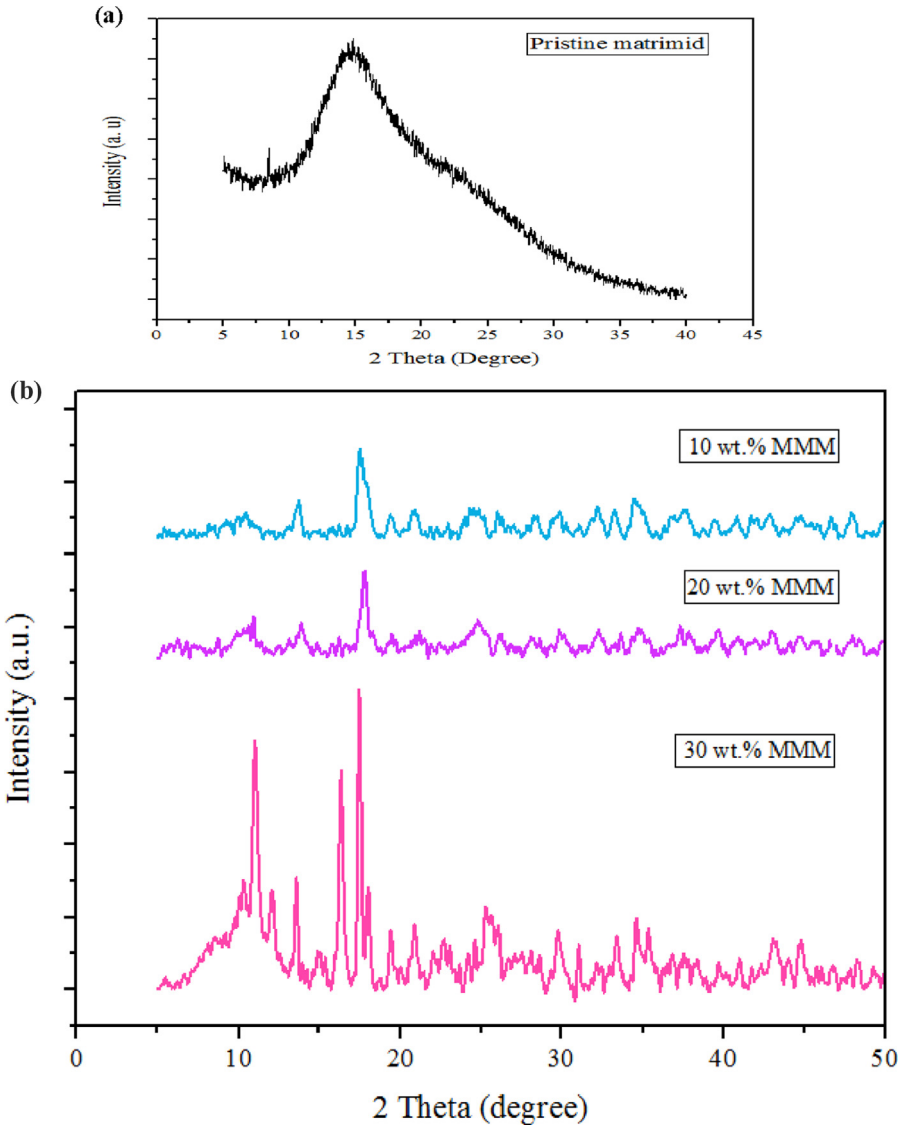

Fig. 6 PXRD of Pure Matrimid membrane (a), MMM with 10 wt%, 20 wt% and 30 wt% MOF (b).

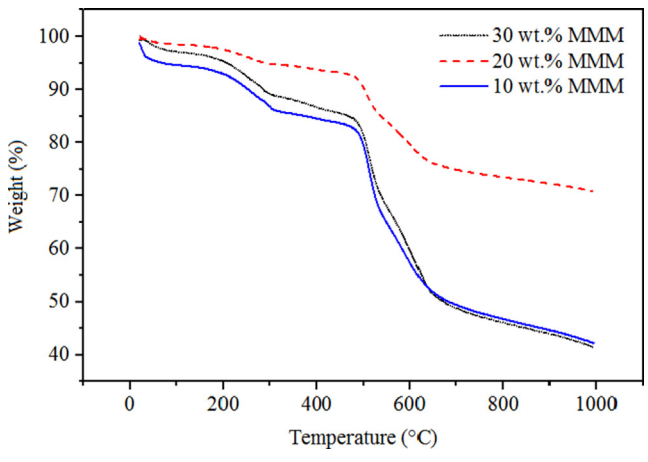

Fig. 7 Thermograms for MMM with 10, 20 wt% and 30 wt% loading of MOF.

3.3. Gas separation studies

The gas separation performance of pure components and mixed gases i.e. CO_2 and CH_4 was evaluated at isochoric conditions and at standard temperature i.e. 25 °C. The kinetic diameter of CO_2 is smaller than CH_4 (Song et al., 2012). The entire course of gas separation experiments was carried out by using the perfectly dried membranes while three coupons were obtained from each composition of the membrane. These membrane modules were set in the permeation cell for gas separation studies. Each membrane sample was subjected to the permeability measurements thrice and an average of these permeability values was used.

The single component CO_2 and CH_4 gas permeabilities (Fig. 9) were noted to be 7.24 and 0.2 Barrer respectively that was quite similar to previously reported data in literature (Hsieh et al., 2014). The permeability values was observed to be increased with the addition of $[Tb(BTC)(H_2O).(DMF)_{1.1}]$ as filler in the Matrimid® 5218. The interactions present

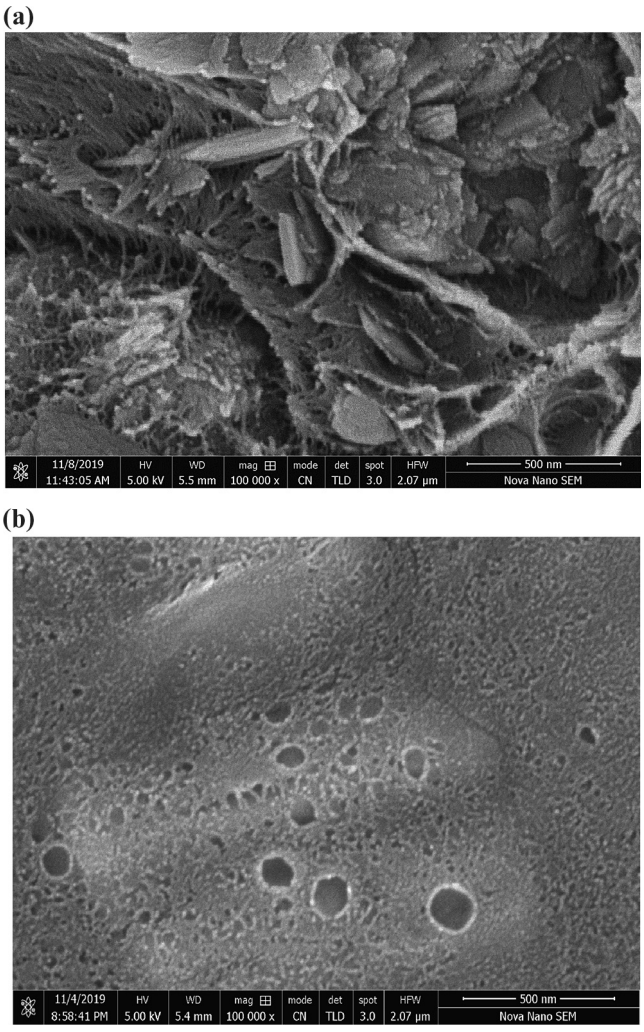

Fig. 8 Cross sectional SEM images of 10 wt% MMM with 500 nm resolution (a) SEM images of surface of 10 wt% MMM with 500 nm resolution (b).

between the polar groups of Matrimid ® 5218 and CO_2 as well as its high degree of condensability caused increase in its permeability through the membrane. Hence, pristine Matrimid proved to be an efficient membrane module for CO_2 permeability.

The incorporation of MOF in to the Matrimid®5218 caused a positive influence on the permeability of CO_2 through the obtained membrane module. Furthermore, an increase in the filler amount caused a positive impact on the permeability of pure CO_2 through the resulting MMMs. The permeability of MMMs with 10 wt% loading of MOF was found to be 13.2 Barrer for CO_2 while the permeability of MMMs with 20 and 30 wt% loadings was improved to 18.34 and 25.86 Barrer respectively for this gas. The good permeability of CO_2 through the Pure Matrimid and all of the three MMMs may be attributed to the smaller kinetic diameter of CO_2, its polar nature, and creation of significant interactions between the CO_2 molecules and the polar groups present in the Matrimid structure. These are the factors which actually define a membrane's potential for gas separation. Furthermore, good compatibility and adhesion of filler with Matrimid matrix are also

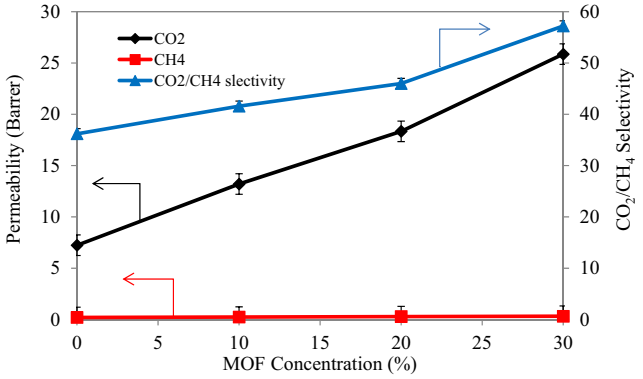

Fig. 9 Pure CO_2 and CH_4 permeabilities and selectivities.

hypothesized to play their roles as it is mentioned previously in literature (Dorosti et al., 2014).

The permeability of the pristine Matrimid was not significantly increased for CH_4 as compared to CO_2 gas as the kinetic diameters of both the gases were different. The incorporation of the filler into the Matrimid matrix also led to slight increase in permeability of CH_4. Moreover, the permeability of CH_4 through MMMs was observed to be increased with an increase in the percent loadings of the filler, however this increase was not so pronounced.

Also the permeability of the MMM was found to be higher for CO_2 gas as compared with the CH_4 gas. It was attributed to the fact that smaller kinetic diameter of CO_2, its polar nature, and possibility of good interaction between the filler and CO_2 gas molecules would render the mixed matrix membrane modules to be good choice for separation of CO_2 (Abedini et al., 2014). The incorporation of the porous fillers created the easy transport channels for the faster diffusion of CO_2.

The pure gas component selectivity of CO_2/CH_4 was improved on the addition of the filler in the Matrimid matrix. The selectivity value of 41.58 was obtained for MMM with 10 wt% loading that accounted for a 14.86% increase in selectivity than pristine Matrimid. The selectivity was also found to be increased with the increased filler loading. The MMM with 20 wt% loading of filler offered a selectivity of 46 for the CO_2/CH_4 gas pair. The highest selectivity of 57.21 was observed for MMM with 30 wt% loading of filler which represented a 58.04% increase in selectivity over the pristine Matrimid membrane. This increase in selectivity is explained on the basis of the molecular sieving effect of the filler as well as the difference in molecular sizes of both gases.

The increase in selectivity and permeability simultaneously for all the penetrant gases evidenced the good selection of the polymer-filler pair which resulted in a defect free MMMs.

The diffusion coefficients of each component gas may be used to explain the enhanced selectivity and permeability of the penetrant gases. An increase in diffusion coefficient of pure CO_2 gas molecules was observed for the MMM with 10 wt% loading than the pure matrimid membrane as depicted in Fig. 10. The permeability of the penetrant gases was increased significantly on filler incorporation into the Matrimid matrix that is explained due to the increased diffusion of gas molecules through the larger pores of the filler. On increasing the filler loading, a concomitant increase in the diffusion coefficient of the gas molecules was observed as the larger pores

of the filler are greater in number than the free volume elements of the polymer matrix that eased the flow of gas molecules through the membranes (Winberg et al., 2005).

The diffusivity of a gas is affected by the shape, pore size of filler and its flexibility. The diffusion coefficient of CO_2 was found to increase with a concomitant increase in filler loading for all of the MMMs modules. However in case of CH_4, the diffusion co-efficient was no increased significantly that is attributed to the week interactions between the CH_4 molecules and the filler pores as well as the larger size of penetrant CH_4 gas.

The influence of filler incorporation on the gas transport behavior through the prepared MMMs is evaluated in terms of Facilitation ratio. Facilitation ratio is the difference of permeability of the composite and pure polymer divided by the permeability of pure polymer. It is a preferred tool to evaluate the influence of filler incorporation on the behavior of gas transport in the prepared MMMs. The Fig. 11 elaborates the facilitation ratios of CH_4 (3.8 Å) and CO_2 (3.3 Å) (Tahir et al., 2018) through $[Tb(BTC)(H_2O).(DMF)_{1.1}]$/ Matrimid MMMs with different filler loadings. The introduction of the porous filler in the MMMs may create a permanent porosity in MMMs that resulted in an increased gas permeability and thus possibly increasing the facilitation ratio.

The industrial applicability of the fabricated membrane modules was evaluated by using a 50:50 feed compositions of CH_4 and CO_2. The membrane modules with different filler loadings exhibited the same trend for separation efficiency,

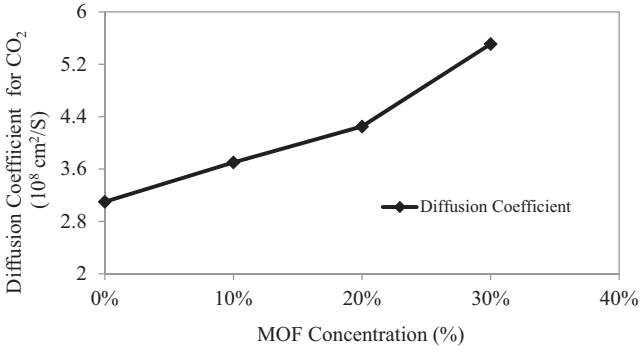

Fig. 10 Solubility and diffusitivity coefficients of Pristine Matrimid and MMMs.

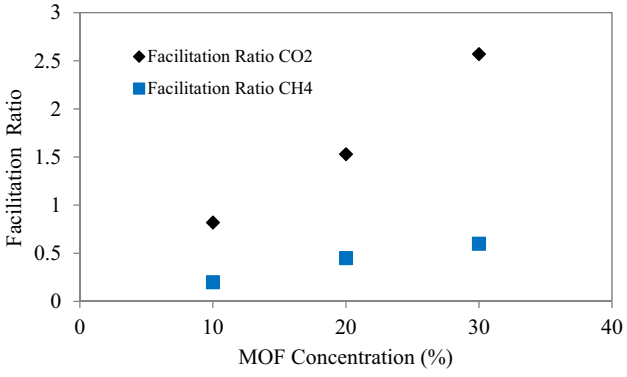

Fig. 11 Facilitation ratio of CO_2, CH_4 for MMMs.

the selectivity and permeability values were found to increase with an increased filler loading as shown in the Fig. 12. However, the selectivity of mixed gases were slightly less than the pure gas separation of CH_4 and CO_2 probably that may be explained on the basis of competitive sorption effect.

In addition to the larger size of CH_4 gas molecules, the permeation of CO_2 molecules through the membrane module is also hindered due to the plasticization effect of the penetrating gas molecules so, reduced selectivity and permeabilities were obtained in comparison with the permeation of pure CO_2. On the other hand, the condensability of CO_2 molecules is reduced by CH_4 and hence the reduced selectivity for this gas pair was observed (Khan et al., 2012b).

The feed composition of CO_2 was varied under the conditions of constant temperature of 298 K and pressure of 10 Bars and the separation factor for CO_2/CH_4 gas pair was determined. The corresponding data is provided in Fig. 13. The Fig. 13 depicted a decreased selectivity of CO_2 with its increased feed concentration for the pure Matrimid membrane while MMM with 10 wt% loading of filler followed the trend that is quite similar to the previously published one (Basu et al., 2010a). Although, the overall selectivity of the MMMs was increased by increasing the filler concentration but, the separation factor may decrease due to the presence of higher CO_2 content as reported earlier (Basu et al., 2010a, Härtel and Püschel, 1999; David et al., 2011). The interaction of CO_2 with the polar groups of the Matrimid may cause the swelling of polymer matrix which in turn may increase the free volume and the mobility of the polymer chains (Ahn et al., 2008). So, the permeation of the penetrant gases was increased as facilitated by the polymer chain relaxation that resulted in a less selective transport through the membrane that was exposed to higher CO_2 concentration. The competitive sorption is found to be mainly responsible for the depression in selectivity as all of the experiments were performed at pressure of 10 Bars that is actually very lower than the plasticization pressure of the Matrimid membranes (Khan et al., 2012b). A slightly reduced CO_2/CH_4 selectivity was observed for the pristine Matrimid membrane as compared to all the other MOF loaded MMMs due to incorporation of porous filler in the MMMs which offered extra transport channels in the MMMs to offer reduced depression in selectivity as a result of high concentrations of CO_2.

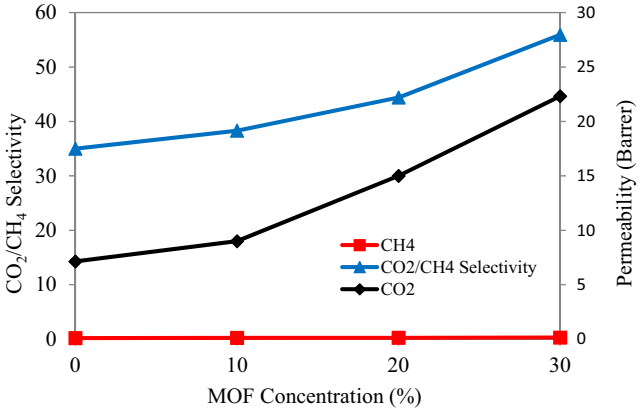

Fig.12 Effect of different concentrations of MOF loadings on the CO_2/CH_4 selectivity.

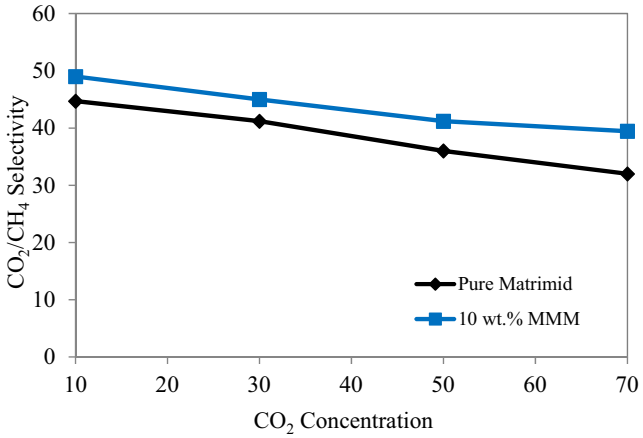

Fig. 13 Membrane modules permeability performances under different concentrations of CO_2.

Fig. 14 depicts the influence of feed temperature on the permeability of pristine Matrimid and MMMs modules as recorded by varying the temperature between 298 K and 338 K. In the case of pristine Matrimid module, the permeability of penetrant gases was found to be increased with an increase in temperature. It was explained on the basis of fact that at higher temperatures the polymer chains become more flexible and thus they offer more fractional free volume resulting in an improved diffusion with increased temperature and the previous literature also supports our findings (Tahir et al., 2018). The MMMs modules also followed the same trend but with some improved permeabilities. The porous nature of incorporated filler renders addition pathways for transport of gases that facilitated the CO_2 transport thereby improving the molecular flow and hence diffusion. The relationship between the gas permeability and operating feed is well explained by Arhenius equation as given below:

$$P = P_o \exp\left(\frac{-EP}{RT}\right) \quad (9)$$

where permeability is denoted by P, P_o represents pre-exponential factor. T is the absolute feed temperature and R being the gas constant.

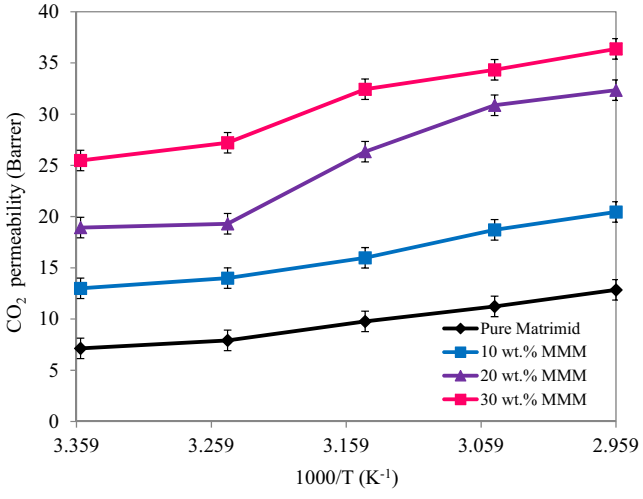

Fig. 14 Temperature effect on permeability of membranes.

The selectivity of pristine Matrimid and the MMM module with 10 wt% loading of filler as a function of temperature is depicted in Fig. 15. The temperature was varied in the range of 298 K to 338 K. An increased temperature was noted to cause a decrease in selectivity of pristine Matrimid membrane. However the selectivity was increased in MMMs with the increasing concentration of the filler. In general, the flexibility of the polyimide chains is increased at high temperatures which may improve the diffusion of gas molecules through their membrane modules (Khan et al., 2010). In contrast to the permeability, the decreased selectivity was explained on the basis of non-compliance of size exclusion phenomena for the binary gas pair CO_2/CH_4 by the membrane modules as the polymer chains were relaxed at higher temperatures. So, the diffusivity was enhanced at the expense of separation factor for CO_2 (Tahir et al., 2018).

3.4. Robeson's upper bound

In order to elucidate its industrial importance of the fabricated MMMs for efficiency based performance, their full potential was compared with famous Robeson Upper Bound 2008 as depicted in Fig. 16. It is apparent from the Fig. 16 that with the increased filler loading of the membrane modules, they

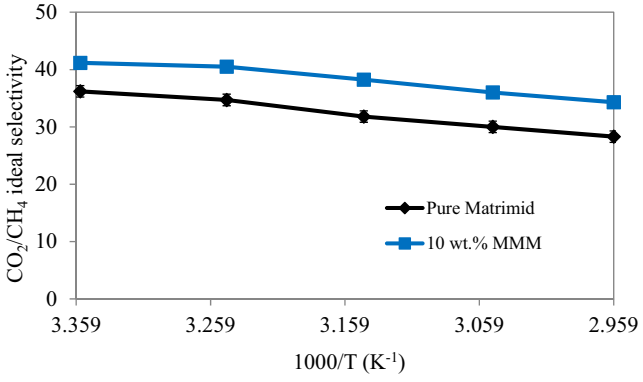

Fig. 15 Effect of temperature on selectivity of pure Matrimid as well as MMMs with various MOF loadings.

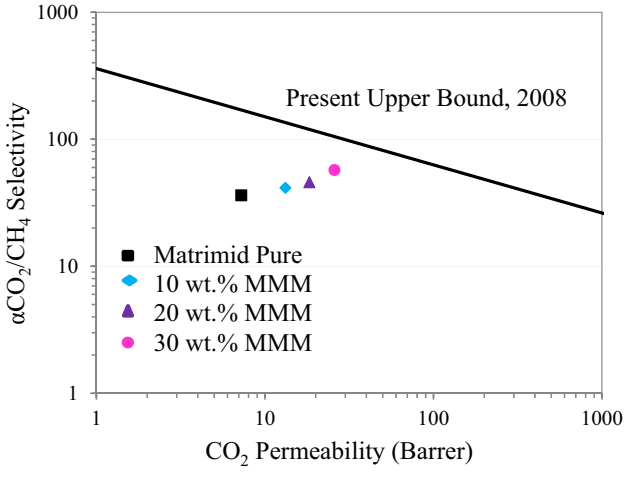

Fig. 16 Robeson's Upper Bound for pure Matrimid and the MMMs fabricated in this work.

Table 1 Comparison of results of current study with some reported data.

Filler	Optimum Loading (wt, %)	Operating temperature (°C) and Pressure (Bar)	P(CO_2) Barrer	CO_2/CH_4 Selectivity	Ref.
MIL-53	30	35, 3	7.5	46	Dorosti et al 2015
MIL-53	15	35, 3	12.43	51.8	Dorosti et al 2014
ZIF-8	30	25, 8	33.1	15.4[a]	Castro – Muñoz et al 2019
MOF-5	10	35, 2	11.1	50.5	Perez et al 2009
$Cu(BTC)_3$	5	–	7.5	21	Basu et al., 2010b
$Tb(BTC)(H_2O).(DMF)_{1.1}$	30	25, 10	25.86	57.21[b]	Present study
$Tb(BTC)(H_2O).(DMF)_{1.1}$	30	25, 10	22.32	55.91[a]	Present study

[a] Binary mixture (50:50) of gases was used.
[b] Pure gas was used.

approached quite closer to the upper bound. So the MMM with 30 wt% loading of the filler was found to be the most efficient membrane module but still it is little far from the Upper bound 2008. The good efficiency of the membrane module for the separation of CO_2 from CH_4 was due to the porous nature of the MOF used in this study.

3.5. Comparison with literature

The MMMs of the present study were compared with some reported Matrimid based MMMs containing promising MOFs like ZIF-8, MIL-53, $Cu(BTC)_3$ and MOF-5. The corresponding data is provided in Table 1, that depicted the MMM prepared in present study with highest MOF loading as the best performing one. Although, this membrane has not surpassed the Robeson's upper bound of 2008, but the selectivity values for the CO_2/CH_4 pairs were closer to the upper bound. In conclusion, the 30 wt% MOF loaded membrane was found to be the most efficient one over the pure Matrimid 10 and 20 wt% MMMs prepared in this work and some other MOFs loaded MMMs.

4. Conclusions

The industrial applicability of the fabricated 10, 20 and 30 wt % $Tb(BTC)(H_2O).(DMF)_{1.1}$/Matrimid®5218 MMMs was evaluated. The incorporation of this MOF as a filler into the Matrimid led to an increase in permeability of CO_2 which was increased with an increase in concentration of this filler in the Matrimid.

The permeability of CH_4 was increased slightly as compared to CO_2 in pristine Matrimid due to size exclusion phenomena. The filler incorporation into the Matrimid matrix also increased the pure gas selectivity of CO_2 /CH_4. The increased values of selectivity and permeability for all penetrant gases especially CO_2 to a much greater extent as compared with CH_4 proved that polymer – filler pair was right selection for the formation of defect free MMMs. An increase in filler loading was associated with increased facilitation ratio of CO_2 and CH_4. The selectivity of the mixed gas components was slightly lower than the pure gases as governed by competitive sorption effect and plasticization due to gases.

The presence of high CO_2 feed concentration caused non – selective transport due to swelling of polymer resulting from improved free volume and the mobility of polymer chain. This leads to a great depression in selectivity. At high temperatures, the increased filler loading improved the selectivity due to porous nature of filler as well as the extra transport pathways offered by the use of non – modified filler.

The comparison of selectivity and permeability of CO_2 for presently fabricated MMMs with previous studies revealed that the prepared membranes were sufficiently promising towards separation of CO_2 and CH_4 using this filler – polymer pair. Whereby, the non– modified porous filler offered high diffusion and sorption of gases whilst the intrinsic properties of $Tb(BTC)(H_2O).(DMF)_{1.1}$ offered efficiently improved performance of the designed MMMs. The gas separation results obtained proved promising industrial applicability of Tb $(BTC)(H_2O).(DMF)_{1.1}$ MOF.

5. Funding**a

This work was sponsored by the Higher Education Commission of Pakistan [Grant number 1 – 8/HEC/HRD/2017/7988] that was availed for *Facultät fur Chemie und Pharmazie, ANORGANISHE CHEMIE, Julius-Maximilians-UNIVERSITÄT WÜRZBURG.*

6. Contributions**a

All authors have contributed significantly towards this study.

Declaration of Competing Interest

The authors declare that they have no known competing financial interests or personal relationships that could have appeared to influence the work reported in this paper.

Acknowledgments

We are thankful to Institute of Chemistry, University of the Punjab, Lahore, Pakistan as all research work was performed here. We acknowledge the funding received by HEC as this work was sponsored by the Higher Education Commission of Pakistan [Grant number 1 – 8/HEC/HRD/2017/7988].

References

Abdulhameed, M.A., Othman, M.H.D., Ismail, A.F., Matsuura, T., Harunm, Z., Rahman, M.A., Hubadillah, S.K., 2017. Carbon dioxide capture using a superhydrophobic ceramic hollow fiber membrane for gas-liquid contacting process. J. Clean. Prod. 140, 1731–1738.

Abedini, R., Omidkhah, M., Dorosti, F., 2014. Highly permeable poly (4-methyl-1- pentyne)/NH2-MIL.53 (Al) mixed matrix membrane for CO2/CH4 separation. RSC Adv. 4, 36522–36537.

Ahmad, J., Hägg, M.-B., 2013. Development of matrimid/zeolite 4A mixed matrix membranes using low boiling point solvent. Sep. Purif. Technol. 115, 190–197.

Ahn, J., Chung, W.J., Pinnau, I., Guiver, M.D., 2008. Polysulfone/silica nanoparticle mixed-matrix membranes for gas separation. J. Membr. Sc.i 314, 123–133.

Anjum, M.W., Vermoortele, F., Khan, A.L., Bueken, B., De Vos, D. E., Vankelecom, I.F.J., 2015. Modulated UiO–66 based Mixed Matrix Membranes for CO_2 Separation. ACS Appl. Mater. & interfaces 7, 25193–25201.

Ariazadeh, M., Farashi, Z., Azizi, N., Khajouei, M., 2020. Influence of functionalized SiO_2 nanoparticles on the morphology of CO_2/CH_4 separation efficiency of Pebax – based mixed matrix membranes. Korean J. Chem. Eng. 37, 295–306.

Basu, S., Cano-Odena, A., Vankelecom, I.F.J., 2010a. Asymmetric membrane based on Matrimid and polysulphone blends for enhanced permeance and stability in binary gas (CO_2/CH_4) mixture separations. Sep. Purif. Technol. 75, 15–21.

Basu, S., Cano-Odena, A., Vankelecom, I.F., 2010b. Asymmetric Matrimid®/ $[Cu_3(BTC)_2]$ mixed-matrix membranes for gas separations. J. Membr. Sci. 362, 478–487.

Boroglu, M.S., Ugur, M., Boz, I., 2017. Enhanced gas transport properties of mixed matrix membranes consisting of Matrimid and RHO type ZIF – 12 particles. Chem. Eng. Res. Des. 123, 201–213.

Castro-Muñoz, R., Fíla, V., Martin-Gil, V., Muller, C., 2019. Enhanced CO_2 permeability in Matrimid® 5218 mixed matrix membranes for separating binary CO_2/CH_4 mixtures. Sep. Purif. Technol. 210, 553–562.

Castruita-de León, G., Yeverino-Miranda, C.Y., Montes-Luna, A.-G. J., Meléndez-Ortiz, H.I., Alvarado-Tenorio, G., García-Cerda, L. A., 2020. Amine – Impregnated natural zeolite as filler in mixed matrix membranes for CO_2/CH_4 separation. Appl. Polym. Sci. 137, 48286.

Chung, T.S., Jiang, L.Y., Li, Y., Kulprathipanja, S., 2007. Mixed matrix membranes (MMMs) comprising organic polymers with dispersed inorganic fillers for gas separation. Prog. Polym. Sci. 32, 483–507.

Cota, I., Martinez, F.F., 2017. Recent advances in the synthesis and applications of metal organic frameworks doped with ionic liquids for CO_2 adsorption. Coord. Chem. Rev. 351, 189–204.

David, O.C., Gorri, D., Urtiaga, A., Ortiz, I., 2011. Mixed gas separation study for the hydrogen recovery from $H_2/CO/N_2/CO_2$ post combustion mixtures using a Matrimid membrane. J. Membr. Sci. 378, 359–368.

Davis, M.E., 2002. Ordered Porous Materials for Emerging Applications. Nature. 417, 813–821.

Dorosti, F., Omidkhah, M., Abedini, R., 2014. Fabrication and characterization of Matrimid/MIL – 53 mixed matrix membrane for CO_2/CH_4 separation. Chem. Eng. Res. Des. 92, 2439–2448.

Dorosti, F., Omidkhah, M., Abedini, R., 2015. Enhanced CO_2/CH_4 separation properties of asymmetric mixed matrix membrane by incorporating nano – porous ZSM – 5 and MIL – 53 particles into Matrimid® 5218. J. Nat. Gas Sci. Eng. 25, 88–102.

Feng, X., Zhao, J., Liu, B., Wang, L., Ng, S., Zhang, G., Wang, J., Shi, X., Liu, Y., 2010. A Series of Lanthanide–Organic Frameworks Based on 2 – Propyl-1H – imidazole – 4, 5 – dicarboxylate and Oxalate: Syntheses, Structures, Luminescence, and Magnetic Properties. Cryst. Growth. Des. 10, 1399–1408.

Galiatsatou, P.P., Kanellopoulos, N.K., Petropoulos, J.H., 2006. Characterization of the transport properties of membranes of uncertain macroscopic structural homogeneity. J. Membr. Sci. 280, 634–642.

Goh, P.S., Ismail, A.F., Sanip, S.M., Ng, B.C., Aziz, M., 2011. Recent Advances of Inorganic Fillers in Mixed Matrix Membrane for Gas Separation. Sep. Purif. Technol. 81, 243–264.

Guo, X.D., Zhu, G.S., Li, Z.Y., Sun, F.X., Yang, Z.H., Qiu, S.L., 2006. A lanthanide metal-organic framework with high thermal stability and available Lewis – acid metal sites. Chem. Comm. 30, 3172–3174.

Härtel, G., Püschel, T., 1999. Permselectivity of a PA6 membrane for the separation of a compressed CO_2/H_2 gas mixture at elevated pressures. J. Membr. Sci. 162, 1–8.

He, X., Kim, T.-J., Hägg, M.-B., 2014. Hybrid fixed-site-carrier membranes for CO_2 removal from high pressure natural gas: Membrane optimization and process condition investigation. J. Membr. Sci. 470, 266–274.

He, X., Chu, Y., Lindbrathen, A., Hillestad, M., Hagg, M.B., 2018. Carbon molecular sieve membranes for biogas upgrading: techno-economic feasibility analysis. J. Clean. Prod. 194, 584–593.

Hsieh, J.O., Balkus, K.J., Ferraris, J.P., Musselman, I.H., 2014. MIL – 53 frameworks in mixed – matrix membranes. Micro. Mesoporous Mater. 196, 165–174.

Hua, Y., Wang, H., Li, Q., Chen, G., Liu, G., Duan, J., Jin, W., 2018. Highly efficient CH_4 purification by LaBTB PCP – based mixed matrix membranes. J. Mater. Chem. A 6, 599–606.

Hu, Z., Kang, Z., Qian, Y., Peng, Y., Wang, X., Chi, C., Zhao, D., 2016a. Mixed Matrix Membranes Containing UiO-66(Hf)-$(OH)_2$ Metal–Organic Framework Nanoparticles for Efficient H_2/CO_2 Separation. Ind. Eng. Chem. Res. 55, 7933–7940.

Hu, Z.G., Nalaparaju, A., Peng, Y.W., Jiang, J., Zhao, D., 2016b. (b). Modulated Hydrothermal Synthesis of UiO – 66 (Hf) – $(OH)_2$ – Type Metal Organic Frameworks for Optimal CO_2 Separation. Inorg. Chem. 55, 1134–1141.

Hu, Y., Zhang, J., Hou, H., Wang, Z., Xu, X., Yang, Y., Lin, K., Fan, R., 2020. One – pot synthesis of bimetallic metal organic frame works (MOFs) as acid base bi – functional catalysts for tandom reaction. Catal. Sci. Technol. 10, 315–322.

Ismail, A.F., Rana, D., Matsuura, T., Foley, H.C., 2011. Carbon-based membranes for separation processes. Springer Science & Business Media.

Jiang, H.-L., Tsumori, N., Xu, Q., 2010. A series of (6, 6) – connected porous Lanthanide – Organic frame works eantiomers with high thermostability and exposed metal sites: scalable syntheses, structures and sorption sites. Inorg. Chem. 49, 10001–10006.

Johannas, W.M., Osterrieth, Fairen – Jimenez, D., 2020. Metal organic frame work composites for Theragnostics and drug delivery applications. Biotechnol. J. 2000005.

Khan, A.L., Basu, S., Cano – Odena, A., Vankelecom, I.F.J., 2010. Novel high throughput equipment for membrane-based gas separations. J. Membr. Sci. 354, 32–39.

Khan, M.M., Filiz, V., Bengtson, G., Shishatskiy, S., Rahman, M., Abetz, V., 2012a. Functionalized Carbon Nanotubes Mixed Matrix Membranes of Polymers of Intrinsic Microporosity for Gas Separation. Nanoscale Res. Lett. 7, 504–516.

Khan, A.L., Klaysom, C., Gahlaut, A., Li, X., Vankelecom, I.J.F., 2012b. SPEEK and functionalized mesoporous MCM – 41 mixed matrix membranes for CO_2 separations. J. Mater. Chem. 22, 20057–20064.

Kertik, A., Wee, L.H., Pfannmöller, M., Bals, S., Martens, J.A., Vankelecom, I.F.J., 2017. Highly selective gas separation membrane using in – situ amorphised metal – organic frameworks. Energy & Environ. Sci. 10, 2342–2351.

Kim, Y.S., Kusakabe, K., Morooka, S., Yang, S.-M., 2001. Preparation of microporous silica membranes for gas separation. Korean Chem. Eng. 18, 106–112.

Li, J.-R., Ma, Y., McCarthy, M.C., Sculley, J., Yu, J., Jeong, H.-K., Balbuena, P.B., Zhou, H.-C., 2011. Carbon Dioxide Capture-Related Gas Adsorption and Separation in Metal-Organic Frameworks. Coord. Chem. Rev. 255, 1791–1823.

Li, T., Pan, Y., Peinemann, K.-V., Lai, Z., 2013. Carbon dioxide selective mixed matrix composite membrane containing ZIF-7 nano-fillers. J. Membrane Sci. 425–426, 235–242.

Li, W., Pan, F., Song, Y., Wang, M., Wang, H., Walker, S., Jiang, Z., 2017. Construction of molecule-selective mixed matrix membranes with confined mass transfer structure. Chin. J. Chem. Eng. 25, 1563–1580.

Lian, X., Zhou, Y.-J., Zhang, H.F., Li, M., Huang, X.-C., 2020. Luminescence turn – on detection by an entanglement – protected MOF operating via a divided receptor – transduecer protocol. J. Mater. Chem. C. 8, 3622–3625.

Liu, C., McCulloch, B., Wilson, S.T., Benin. A.I., Schott, M.E., 2009. Metal organic framework – polymer mixed matrix membranes. US Patent 7637983B1.

Liu, J., Hua, D., Zhang, Y., Japip, S., Chung, T.S., 2018. Precise Molecular Sieving Architectures with Janus Pathways for Both Polar and Nonpolar Molecules. Adv. Mater. 30, 1705933.

Luo, J., Xu, H., Liu, Y., Zhao, Y., Daemen, L.L., Brown, C., Timofeeva, T.T., Ma, S., Zhou, H.-C., 2008. Hydrogen adsorption in a highly stable porous rare-earth metalorganic framework: Sorption properties and neutron diffraction studies. J. Am. Chem. Soc. 130, 9626–9627.

Łyszczek, R., 2007. Thermal and spectroscopic investigations of new lanthanide complexes with 1, 2, 4 – benzenetricarboxylic acid. J. Therm. Anal. Calori. 90, 533–539.

Łyszczek, R., Rzączyńska, Z., Kula, A., Gładysz-Płaska, A., 2011. Thermal and luminescence characterization of lanthanide 2,6-naphthalenedicarboxylates series. J. Anal. Appl. Pyroly. 92, 347–354.

Łyszczek, R., Mazur, L., Ostasz, A., Bartyzel, A., Głuchowska, H., 2017. Lanthanide metal–organic frameworks: Structural, thermal and sorption properties. Special Collection – 15th Ukrainian-Polish Symposium 35, 677–683.

Mannan, H.A., Mukhtar, H., Murugesan, T., Nasir, R., Mohshim, D. F., Mushtaq, A., 2013. Recent Applications of Polymer Blends in Gas Separation Membranes. Chem. Eng. Technol. 36, 1–10.

Marti, A., Venna, S., Roth, E.A., Culp, J.T., Hopkinson, D.P., 2018. A Simple Fabrication Method for Mixed Matrix Membranes with In-situ MOF Growth for Gas Separation. ACS Appl. Mater. Interfaces 10, 24784–24790.

McGuire, C.V., Forgan, R.S., 2015. The Surface Chemistry of Metal-Organic Frameworks. Chem. Commun. 51, 5199–5217.

Moghadam, F., Kamio, E., Yoshioka, T., Matsuyama, H., 2017. New approach for the fabrication of double-network ion-gel membranes with high CO_2/N_2 separation performance based on facilitated transport. J. Membrane Sci. 530, 166–175.

Mubashir, M., Fong, Y.Y., Keong, L.K., Sharrif, M.A.B., 2015. Synthesis and performance of deca-dodecasil 3 rhombohedral (ddr)-type zeolite membrane in CO_2 separation–a review. ASEAN J. Chem. Eng. 2, 48–57.

Mubashir, M., Yeong, Y.F., Chew, T.L., Lau, K.K., 2017. Issues and Current Trend of Hollow Fiber Mixed Matrix Membranes for CO_2 Separation from N_2 and CH_4. Chem. Eng. Technol. 41, 235–252.

Ordoñez, M.J.C., Balkus Jr, K.J.B., Ferraris, J.P., Musselman, I.H., 2010. Molecular sieving realized with ZIF – 8/Matrimid® mixed-matrix membranes. J. Membrane Sci. 361, 28–37.

Pall, P., Aina, T., Stone, D.A., Stott, P.A., Nozawa, T., Hilberts, A.G. J., Dag, L., Allen, M.R., 2011. Anthropogenic Greenhouse gas Contribution to flood Risk in England and Whales in Autumn 2000. Nature 470, 382–385.

Perez, E.V., Balkus, K.J., Ferraris, J.P., Musselman, I.H., 2009. Mixed Matrix Membranes containing MOF – 5 for Gas Separtion. J. Membrane Sci. 328, 165–173.

Rehman, A., Farrukh, S., Hussain, A., Pervaiz, E., 2019. Synthesis and effect of metal–organic frame works on CO_2 adsorption capacity at various pressures: a contemplating review. Energy Environ. 31, 367–388.

Rezakazemi, M., Sadrzadeh, M., Matsuura, T., 2018. Thermally stable polymers for advanced high-performance gas separation membranes. Prog. Energy Combust. Sci. 66, 1–41.

Robeson, L.M., 1991. Correlation of separation factor versus permeability for polymeric membranes. J. Membrane Sci. 62, 165–185.

Robeson, L.M., 2008. The upper bound revisited. J. Membrane Sci. 320, 390–400.

Rosi, N.L., Kim, J., Eddaoudi, M., Chen, B., O'Keeffee, M., Yaghi, O. M., 2005. Rod packings and metal-organic frameworks constructed from rod-shaped secondary building unit. J. Am. Chem. Soc. 127, 1504–1518.

Shafeeyan, M.S., Daud, W.M., Shamiri, A.W.A., Aghamohammadi, N., 2015. Modeling of Carbon Dioxide Adsorption onto Ammonia-Modified Activated Carbon: Kinetic Analysis and Breakthrough Behavior. Energy & Fuels 29, 6565–6577.

Shan, M., Seoane, B., Andres-Garcia, E., Kapteijn, F., Gascon, J., 2018. Mixed-matrix membranes containing an azine-linked covalent organic framework: Influence of the polymeric matrix on post-combustion CO_2-capture. J. Membrane Sci. 549, 377–384.

Silva, P., Valente, A.A., Rocha, J., Paz, F.A.A., 2010. Fast microwave synthesis of a microporous Lanthanide – organic frameworks. Cryst. Growth & Des. 10, 2025–2028.

Song, Q., Nataraj, S.K., Roussenova, M.V., Tan, J.C., Hughes, D.J., Li, W., Bourgoin, P., Alam, M.A., Cheetham, A.K., Al-Muhtaseb, S.A., Sivaniah, E., 2012. Zeolitic imidazolate framework (ZIF – 8) based polymer nanocomposite membranes for gas separation. Energy & Environ. Sci. 5, 8359–8369.

Sorribas, S., Zornoza, B., Téllez, C., Coronas, J., 2014. Mixed matrix membranes comprising silica- (ZIF-8) core-shell spheres with ordered meso-microporosity for natural- and bio-gas upgrading. J. Membrane Sci. 452, 184–192.

Tahir, Z., Ilyas, A., Li, X., Bilad, M.R., Vankelecom, I.F., Khan, A.L., 2018. Tuning the gas separation performance of fluorinated and sulfonated PEEK membranes by incorporation of zeolite 4A. J. Appl. Polym. Sci. 135, 45952–45959.

Tin, P.S., Chung, T.S., Liu, Y., Wang, R., Liu, S.L., Pramoda, K.P., 2003. Effects of crosslinking modification on gas separation performance of Matrimid membranes. J. Membrane Sci. 225, 77–90.

Tien-Binh, N., Vinh-Thang, H., Chen, X.Y., Rodrigue, D., Kaliaguine, S., 2015. Polymer functionalization to enhance interface quality of mixed matrix membranes for high CO_2/CH_4 gas separation. J. Mater. Chem. A 3, 15202–15213.

van Krevel, J.W.H., van Rutten, J.W.T., Mandal, H., Hintzen, H.T., Metselaar, R., 2002. Luminescence properties of terbium-, Cerium-, or Europium- doped α- sialon materials. J. Solid State Chem. 165, 19–24.

Venna, S.R., Carreon, M.A., 2011. Amino-Functionalized SAPO-34 Membranes for CO_2/CH_4 and CO_2/N_2 Separation. Langmuir 27, 2888–2894.

Venna, S.R., Carreon, M.A., 2015. Metal organic framework membranes for carbon dioxide separation. Chem. Eng. Sci. 124, 3–19.

Venna, S.R., Lartey, M., Li, T., Spore, A., Kumar, S., Nulwala, H.B., Luebke, D.R., Rosi, N.L., Albenze, E., 2015. Fabrication of MMMs with Improved Gas Separation Properties Using Externally-Functionalized MOF Particles. J. Mater. Chem. A 3, 5014–5022.

Vinoba, M., Bhagiyalakshmi, M., Alqaheem, Y., Alomair, A.A., Pérez, A., Rana, M.S., 2017. Recent progress of fillers in mixed matrix membranes for CO_2 separation: A review. Sep. Purif. Technol. 188, 431–450.

Ward, J.K., Koros, W.J., 2011. Crosslinkable mixed matrix membranes with surface modified molecular sieves for natural gas purification: II. Performance characterization under contaminated feed conditions. J. Membrane Sci. 377, 82–88.

Wang, Y., Zhao, L., Otto, A., Robinius, M., Stolten, D., 2017. A Review of Post-combustion CO_2 Capture Technologies from Coal-fired Power Plants. Energy Procedia 114, 650–665.

Winberg, P., DeSitter, K., Dotremont, C., Mullens, S., Vankelecom, I. F.J., Maurer, F.H.J., 2005. Free volume and interstitial mesopores

in silica filled poly (1-trimethylsilyl-1-propyne) nanocomposites. Macromolecules 38, 3776–3782.

Wolińska-Grabczyk, A., Kubica, P., Jankowski, A., Wójtowicz, M., Kansy, J., Wojtyniak, M., 2017. Gas and water vapor transport properties of mixed matrix membranes containing 13X zeolite. J. Membrane Sci. 526, 334–347.

Yamamoto, M., Kusakabe, K., Hayashi, J.-I., Morooka, S., 1997. Carbon molecular sieve membrane formed by oxidative carbonization of a copolyimide film coated on a porous support tube. J. Membrane Sci. 133, 195–205.

Yang, L., Song, Y., Wang, L., 2020. Multi – emmission Metal Organic Frameworks Composites for Multicomponent Ratiometric Fluorescence Sensing: Recent Developments and Future Challenges. J. Mater. Chem. B 8, 3292–3315.

Zornoza, B., Seoane, B., Zamaro, J.M., Téllez, C., Coronas, J., 2011. Combination of MOFs and zeolites for mixed-matrix membranes. Chem. Phys. Chem. 12, 2781–2785.